Study Of The Influence Of Contact Model Parameters On A Berthing Operation

75th International Astronautical Congress (IAC), Milan, Italy, 14-18 October 2024.

IAC-24-C2.IP41

Study Of The Influence Of Contact Model Parameters On A Berthing Operation

Davide Sorli[a]*, Giulia Calvo[b], Martina Ferrauto[b], Francesca Giardina[b], Mario Troise[b], Stefano Mauro [b]

[a] *Department of Management and Production Engineering, Politecnico di Torino, Torino, Italy*
[b] *Department of Mechanical and Aerospace Engineering, Politecnico di Torino, Torino, Italy*
* Corresponding Author

Abstract

The MUSAPOEM project aims to develop models and architectures for multi-satellite rendezvous, docking and berthing missions in Earth and lunar orbit. The current mission architecture consists of a target satellite, a chaser satellite, a monitoring satellite and a communication satellite. The chaser maneuvers to approach the target to a separation of a few centimeters, then the target is cached by a robotic manipulator which performs a berthing and docking operation. The ultimate goal of the project is to develop a digital twin of the system, useful for the control during specific phases of the maneuver.

Within different tasks of the project, this paper focuses on the contact mechanics behaviour between the robotic manipulator and the target. A detailed description of contact mechanic can be obtained by FEM and multibody models, which provides a high fidelity representation of the system but are not suitable for real time simulation. For this purpose lumped parameters model are necessary, suitable for real time simulation but representative of a specific phase of the berthing or docking operation. The project methodology involves developing a high-fidelity model and interpreting its results to define lumped parameters models representative of specific mission phases.

This paper discusses the development of a multibody model of the free floating chaser and target satellites, built in Matlab/Simscape environment. In the model a robotic manipulator suitable for the berthing operation is introduced. The geometry of the end effector and the grasped element on the target are defined. A contact model, defined by parameters dependent by materials and the geometry of contacts elements, is introduced to describe contact during the berthing operations. The interaction between the end effector and the target influences the attitude of both satellites, with incorrect material and geometry choices risking the failure of the berthing operation. An analysis of model parameters' influence on the target and chaser satellite attitudes is conducted. Results allow to define a range of parameters which leads to a successful berthing. Results allow also to propose geometries and materials for the end effector and the target. Next steps regard the extrapolation of lumped parameters contact model from the high fidelity analysis.

Keywords: space robotics; berthing; contact mechanics; in orbit servicing

1. Introduction

On orbit servicing missions requires systems and mechanism capable of coupling satellites to perform complex operations such as refuelling, on orbit assembly and repairing. Coupling technologies have been studied and developed since NASA's Gemini missions and have received a new impulse in research and development due to the recent increase of small satellites in space assembly applications [1]. The coupling can be obtained through docking or berthing [2]. Docking refers to the autonomous approach and connection of two spacecraft. It involves the mechanical coupling of both vehicles, where the chaser satellite's guidance, navigation, and control (GNC) system regulates the relative positioning between the two bodies. The GNC system ensures proper contact conditions, managing factors like relative misalignment and velocity. In this process, the capture point is also where the structural connection is established [3]

Berthing define a manual or remotely assisted capture and attachment performed by a robotic manipulator installed on one of the satellites. A space robotic system (also referred to as space manipulator or space robot) for an IOS mission typically consists of three major components: the base spacecraft (or servicing satellite), an n degree-of-freedom (n-DOF) robot manipulator attached to the servicing satellite, and the target spacecraft to be serviced [4].

The first robotic arm used in space application is the Canadarm-1 [5]. It demonstrated the usefulness of robotic systems in space and led to the development of the Canadarm-2 [6], the first redundant manipulator for space use.

Other successful applications include the JEM Remote Manipulation System, equipped on the Japanese Experiment module and specifically designed to support experiments on the JEM Exposed Facility [7], and the 7-DOFs European Robotic Arm developed by ESA and installed on the ISS [8].

In recent years the focus on the development of space robotic missions has shifted to applications for in orbit

assembly and servicing performed by autonomous systems [9].

NASA OSAM-1 mission demonstrated the capability of in orbit assembly of a satellite communication antenna performed by a robotic arm (SPIDER) [10]. The mission has been reviewed in 2022 [11].

OSAM-1 should have been followed by OSAM 2 mission [12], designed for on orbit manufacturing and provided with a 7-DOFs manipulator designed by Motiv Space Systems [13]. However, OSAM-2 mission was cancelled due delays and extra-costs.

Exists examples of robotic systems proposal to perform on orbit operations that apply soft robotics system: a proposal for debris removal application can be found in [14], and exists proposal for on board cooperative applications [15]

To design robotics system to perform berthing operations it is useful a tool to describe the dynamics of the systems playing a role during the manoeuvre. In particular, in the case of berthing contact mechanics comprehension plays a crucial role in the description of the manoeuvre, since the interaction between servicer and target is identified in the gripper-interface contact area [16]. Therefore, in the case of space robotics manipulation, the dynamics of the manipulator and of the satellites can be described by the Kane's formulation [17], neglecting celestial mechanics and gravitational forces, so that the bodies can be considered in free floating condition [18].

The contact mechanics description derive from the Hertzian theory [19], where contact forces are described with an elastic model. Applying a spring damper model it can be possible to describe the energy dissipation during the contact [20]. A more precise model is the Hunt-Crossley model [21], which allows to take in account of non-linearities characteristic of plastic deformation and dependent by the material of contact bodies. However, it should be noted that every improvement of the contact model means an higher number of model parameters to be defined and estimated.

In this context, the Italian Space Agency (ASI) funded the MUSAPOEM mission, a multi-satellite initiative aimed at performing autonomous satellite servicing in Earth or lunar orbit. The mission involves a servicer satellite equipped with a robotic arm to operate on a non-cooperative target satellite. A monitoring satellite, equipped with visual servoing systems, oversees the operation, while communication with Earth is maintained through a communication satellite positioned in Earth orbit.

This work presents the architecture of the mission and the design of the robotic system involved. It is presented the end effector and interface design. It is described the control strategy of the manipulator to perform the capture manoeuvre. Particular attention is devoted to the description of the contact mechanics between end effector and interface. A multibody model of the system is developed and through a set of simulations it is identified the influence of contact model parameters on the manoeuvre, to give information on the materials to be used and on the compliance that the mechanism have to ensure.

2. Material and methods

The MUSAPOEM project focuses on studying autonomous berthing and docking operations within a multi-satellite mission scenario. This research examines the case of a berthing operation conducted by a robotic arm mounted on the Servicer satellite (chaser) to engage with a non-cooperative target satellite.

2.1 Robotic Arm physical model

The mission scenario requires to the robotic arm to perform capture and release operations of the target satellite which belong to the category of the small spacecrafts (500kg). The arm is mounted on a bigger servicer (chaser) satellite with a mass of 2000kg. The mission architecture is shown in Fig. *1*

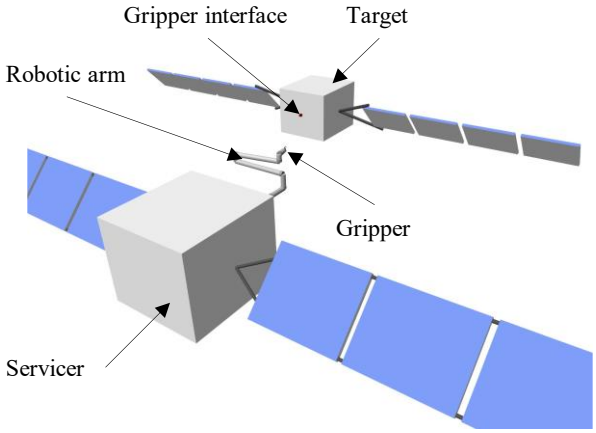

Fig. 1. Architecture of the mission

The robotic arm design is derived from the OSAM-2 mission (cancelled)[12], which involves similar task requirements and satellites sizes. The robotic arm designed is redundant with 7-DOF, the structure is shown in Fig. *2*.

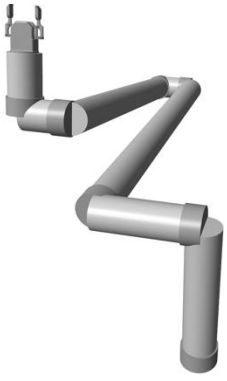

Fig. 2. Robotic arm structure

The mission environment and the robotic arm are modelled in Simscape Multibody™, applying the rigid body model approach.

2.2 End effector model and interface

The design of the end effector is critical for ensuring precise capture of the target satellite. It must maintain continuous contact with the target's interface throughout the entire berthing process. The type of end effector used in space manipulators varies depending on their specific tasks, as well as the size of the manipulator and the satellites involved. For the MUSAPOEM project, the size of the manipulator and the masses of the servicer and target satellites are comparable to missions like OSAM-2, which employs a gripper-type end effector. A gripper end effector has been specifically designed for the MUSAPOEM project. The mechanism's dimensions are selected to generate the required friction force with minimal torque applied by the actuator. On the target side, the interface is modelled as a cube. The design is shown in Fig. *3*

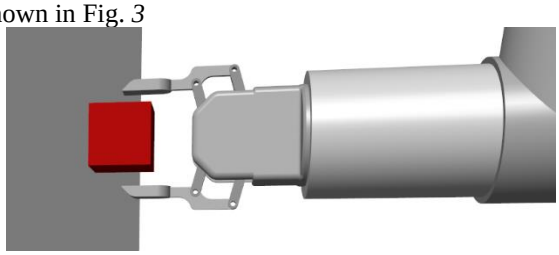

Fig. 3. End effector and interface

3. Theory and calculation

The performance of the robotic arm during the manoeuvre is evaluated considering the attitude of the target satellite and its final attitude error. The attitude of the target depends by the contact mechanics between EE and interface and by the control strategy assigned to the manipulator. This paper describe the contact mechanics model chosen and evaluate the influence of the model parameters on the manoeuvre performed with a given control strategy.

3.1 Contact Mechanics

A precise description of the contact mechanics between the end effector (EE) and the interface is essential for accurately understanding the behavior of the system formed by the two satellites during robotic manipulation maneuvers. Contact mechanics in a space environment is a well-explored topic in the literature, and the choice of a suitable model depends on factors such as the application, simulation conditions, and software used. Employing a multibody approach to simulate and validate these operations is a common practice [22], [23], [24]. The simulation environment used in this work is Simscape Multibody™. In this environment, contact between flexible bodies can be analysed using either built-in models or custom-developed tools [25]. An example of a custom library can be found in [26], where the authors proposed a Simulink library to manage the sphere-groove contact in a ball screw. A similar approach can be used in the further development of the project to more accurately describe the end-effector-interface contact.

One challenge that often arises in contact simulations is the small time step required to calculate contact forces, especially in the case of complex geometries or contact conditions. In this MUSAPOEM project, the entire capture manoeuvre in space, which lasts about 600 seconds, is simulated. Due to the complexity, some simplifications in the contact mechanics are necessary. While the contact between the EE and the interface should ideally be modeled as a plane-plane contact, this approach is computationally expensive. The proposed solution, Fig. *4*, introduces contact proxies in the model, represented as spheres attached to the EE fingers, to simplify the contact to a sphere-plane scenario which significantly improves simulation efficiency and speed

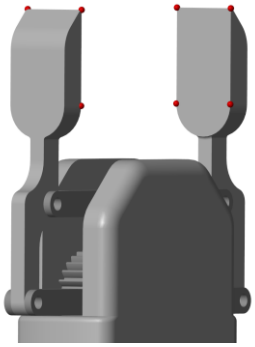

Fig. 4. Contact proxies spheres used to represent the contact mechanic between gripper and interface.

With this simplification, the contact force expressed at the interface is equal to the sum of the forces on the proxies spheres.

The contact model used to calculate the normal contact force includes an elastic component, based on Hertzian contact theory, and a damping component, which accounts for energy dissipation during contact. A third parameter, the contact depth, ensures a continuous damping coefficient throughout the contact, preventing computational issues caused by contact discontinuities[27].

Determining these parameters is challenging, as they depend on the material properties and the geometry of the contact elements. For complex geometries, the contact parameters may vary during the simulation. However, the proposed simplification reduces the problem to a sphere-plane case, where calculating the contact stiffness coefficient becomes straightforward using Hertzian theory[21]:

$$k(q) = \frac{cE_1E_2}{E_1(1-\nu_2^2)+E_2(1-\nu_1^2)}a(q) = c \cdot a(q)E^* \quad (1)$$

Where E_1 and E_2 are the Young's modulus of the contact bodies materials, ν_1 and ν_2 are the Poisson's ratios, c is a load dependent coefficient, 4/3 for the plane-sphere case, a is the radius of the contact surface, function of the radius of the proxy sphere R and of the contact normal force F_n:

$$a = \frac{3F_nR}{4E^*} \quad (2)$$

In this case the normal contact force is dependent by the actuation force given to the end effector clamping mechanism. In a steady state condition its value can be computed with a simple static equilibrium equation. To successfully manipulate the target, the EE must maintain the stiction condition on the grip. To achieve this condition, the friction force F_t at the interface must be equal to the inertia of the target, known because are known the maximum acceleration given by the law of motion and the mass of the satellite. The normal force is computed assuming a friction coefficient of stiction.

With the above assumptions, the open parameters that define the contact mechanic in equation (1) are material dependent, so the objective of this work is to evaluate the influence of the material choice on the capture maneuver.

It is chosen a set of contact stiffness coefficients to evaluate with simulations. In Table 1 are highlighted the set of coefficient chosen, with an indication of the type of contact materials related to the value. However the value is rounded to the power of ten to perform an influence analysis with equally spaced values.

Table 1. Set of stiffness coefficients considered in the sensitivity analysis

	k (N/m)	Contact materials
Case 1	1e3	Aluminum-Elastomer
Case 2	1e4	Polymer-Polymer
Case 3	1e5	Aluminum-Aluminum
Case 4	1e6	Steel-Steel

The damping coefficient is difficult to define because it describe the non-linearity of the plastic deformation. In this study authors chose in a first phase to link the damping coefficient value to the stiffness coefficient decreased by 3 order of magnitude, as suggested by literature references[28], [29]. Identified the optimal stiffness coefficient, it is then evaluated the influence of the damping coefficient.

The friction model is Coulomb-based and modified to ensure that the friction coefficient remains constant throughout the contact. It is defined by three parameters: a dynamic friction coefficient, a stiction friction coefficient, and a critical velocity that determines the maximum friction condition. In the given case, where the contact is predominantly static, the critical velocity is set to a low value of $V_c = 5 \cdot 10^{-4}\, m/s$ to provide an accurate representation of the stiction phase.

3.2 Control Strategy

The MUSAPOEM mission scenario begins with the servicer satellite chasing the target satellite from several kilometers away, ultimately leading to berthing capture. This work focuses on simulating only the final phase of the mission, excluding the processes of target identification, approach, and alignment. Thus, the initial condition for the berthing operation assumes that exist a relative velocity between servicer and target given by the GNC error. However, it is also assumed that this GNC error is not directly measurable and that the maneuver is divided into three stages: first, the robotic arm approaches the target; second, the end-effector (EE) grasps the target; and finally, the servicer and target are joined to complete the berthing operation. The target's identification and pose estimation are carried out using a camera system mounted on the chaser, which provides the target's pose relative to the robot's base. Similar approaches are discussed in [30] and [31]. The servicer's Guidance, Navigation, and Control (GNC) system is supposed to be inactive to energy saving purpose during the maneuver. The robot's joint space state is always available, as it is measured directly by encoders on the joints, and the target's pose is assumed to be continuously available under the assumption that the camera system can reliably identify the target and interface

The desired pose for the end effector, $\boldsymbol{x_s} = [\boldsymbol{p_s}, \boldsymbol{\phi_s}]^T$, is determined using visual servoing. The current pose of the end effector is calculated via forward kinematics given the measured state of the joints. To define the velocity set, both the position and orientation problems must be addressed. The proposed algorithm tackles these issues independently. The position error is calculated as:

$$\boldsymbol{e}_p = \boldsymbol{\Delta p} = \boldsymbol{p}_s - \boldsymbol{p}_{fb} \quad (3)$$

Where $\boldsymbol{p_{fb}}$ is the current position of the target, and $\boldsymbol{p}_s$ is the position to be reached. Based on the position error, the desired velocity of the end effector is determined using a trapezoidal velocity profile. The resulting velocity profile $\dot{\boldsymbol{p}}_s$ is defined as:

$$\dot{\boldsymbol{p}}_s = \min\left(a_o t, v_o, \sqrt{2a_0\|\Delta \boldsymbol{p}\|}\right)\frac{\Delta \boldsymbol{p}}{\|\Delta \boldsymbol{p}\|} \quad (4)$$

a_0 is the maximum acceleration and v_0 is the maximum velocity.

The same approach is used for the solution of the angular problem. With the quaternion representation $\mathcal{Q} = \{\eta, \boldsymbol{\epsilon}\}$, the orientation error $\boldsymbol{e_0}$ is defined as:

$$\boldsymbol{e}_O = \Delta\boldsymbol{\epsilon} = \eta_{fb}(\boldsymbol{q})\boldsymbol{\epsilon}_s - \eta_s\boldsymbol{\epsilon}_{fb}(\boldsymbol{q}) - \boldsymbol{S}(\boldsymbol{\epsilon}_s)\boldsymbol{\epsilon}_{fb}(\boldsymbol{q}) \quad (5)$$

The angular velocity $\dot{\boldsymbol{\phi}}_s$ is computed as a trapezoidal profile:

$$\dot{\boldsymbol{\phi}}_s = \min\left(\alpha_0 t, \omega_o, \sqrt{2\alpha_0\|\Delta\boldsymbol{\epsilon}\|}\right)\frac{\Delta\boldsymbol{\epsilon}}{\|\Delta\boldsymbol{\epsilon}\|} \quad (6)$$

The maximum velocity is set to $\boldsymbol{v_0} = [0.01m/s, 0.01rad/s]$, the maximum acceleration is set to $\boldsymbol{a_0} =$

$[0.005\ m/s^2, 0.005\ rad/s^2]$ for the approaching maneuver and $\boldsymbol{a_0} = [0.0005\ m/s^2, 0.0005\ rad/s^2]$ for the grasping and joining phases. This approach enables the robotic arm to reach the target while compensating for residual GNC velocity errors by assigning a higher acceleration. Additionally, it minimizes reaction forces during the grasping of the target satellite by applying a lower acceleration, which corresponds to reduced inertia.

Using the vector of desired velocities $\boldsymbol{v_s} = [\dot{\boldsymbol{p}}_s, \dot{\boldsymbol{\phi}}_s]^T$, derived from the error $\boldsymbol{e} = [\boldsymbol{e_p}, \boldsymbol{e_O}]^T$, the joint velocities are computed through inverse differential kinematics:

$$\dot{\boldsymbol{q}}_d = \boldsymbol{J}^{\dagger}\boldsymbol{v}_d \quad (7)$$

where:

$$\boldsymbol{J}^{\dagger} = \boldsymbol{J}^T(\boldsymbol{J}\cdot\boldsymbol{J}^T)^{-1} \quad (8)$$

is the right pseudoinverse of the Jacobian matrix *J*. This formulation use the redundancy of the manipulator, provided by its 7th degree of freedom, to locally minimize the norm of the joint velocities[32].

4. Results

The rigid multibody model developed is comprehensive of the robotic arm and of the target and servicer satellites. It is also introduced a dynamic model for the description of joints actuators. The contact mechanics is described with the model presented above. For the development of the simulation tool it is used the Matlab/ Simscape Multibody™ environment.

The influence of the contact model parameters is evaluated with a set of simulations of a berthing operation, Fig. *5*.

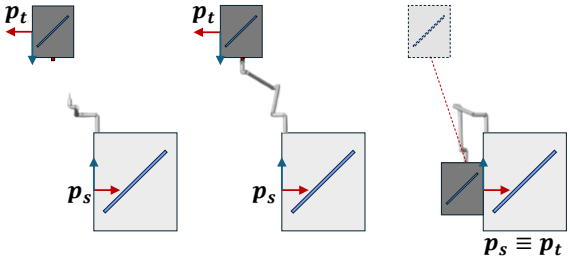

Fig. 5. Phases of the manoeuvre

A first set of simulations has been performed varying the contact stiffness between the values in Table 1. It is evaluated the error between reference frame $\boldsymbol{p_s}$ and $\boldsymbol{p_t}$ which represent the error of the target satellite pose at the end of the manoeuvre. Results are defined with the convention shown in Fig. *6*. It is also evaluated if the contact between the EE and the target is always maintained during the manoeuvre. An uneven contact leads to an imprecise final pose.

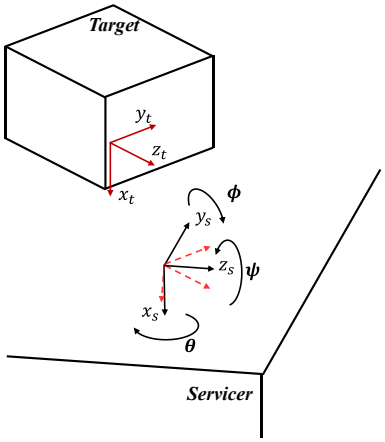

Fig. 6. Definition of servicer and target reference frames

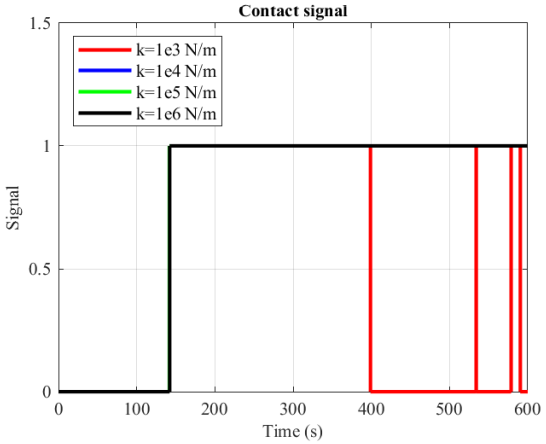

Fig. 7. Contact signal during the manoeuvre

As shown in Fig. *7* the contact is uneven in the case of lower contact stiffness, indicating that the robotic arm has not enough grp on the target.

Table 2. Influence of stiffness coefficient on the measured pose error

	k=1e3 N/m	k=1e4 N/m	k=1e5 N/m	k=1e6 N/m
x [mm]	0.3	0.9	-0.6	-0.3
y [mm]	-19.9	-2.2	-1.5	-1.4
z [mm]	-17.7	-4.7	-5.3	-5.1
θ [rad]	1.23	0.12	5.5e-3	3.5e-3
ϕ [rad]	-0.053	3.9e-3	-2.6e-3	-2.8e-3
ψ [rad]	-0.054	1.3e-3	3.9e-5	6.0e-5

In Table 2 it is shown the measured error. It can be noted that the lower stiffness value, as expected, leads to an high error both in position and orientation. The value of k=1e4 N/m lower the error in position but maintain an high orientation error. Increasing the contact stiffness the

pose error mitigates, with similar results for the k=1e5 N/m and k= 1e6 N/m analysis.

A second set of simulations is performed maintaining the constant value of k=1e5 N/m, similar to the aluminum-aluminum contact case. The damping value is evaluated in the range reported in Table 3

Table 3. Range of contact damping coefficient evaluated

	c (Ns/m)
Case 1	5e0
Case 2	5e1
Case 3	5e2
Case 4	5e3

Results of simulations are reported in Table 4:

Table 4. Influence of damping coefficient on the measured pose error

	c=5 Ns/m	c=50 Ns/m	c=500 Ns/m	c=5000 Ns/m
x [mm]	-0.6	-0.6	-0.6	-0.5
y [mm]	-1.5	-1.5	-1.5	-1.5
z [mm]	-5.3	-5.3	-5.3	-5.3
θ [rad]	5.5e-3	5.5e-3	5.5e-3	5.5e-3
ϕ [rad]	-2.6e-3	-2.6e-3	-2.6e-3	-2.8e-3
ψ [rad]	4.1e-5	5.3e-5	3.9e-5	-4.0e-5

From results of the second set of simulations it can be noted that there is no such influence of the damping coefficient on the resulting target pose error. This results means that the behaviour of the system during the manoeuvre is mainly driven by the elastic component of the contact force, with minor influence of the plastic deformation. This result can be explained with the law of motion imposed to the manipulator, which implicates low velocities and accelerations that leads to low contact deformation velocities, so that the damping component of the contact force is minimized.

5. Conclusions

This work presented the design of a robotic system for performing berthing manoeuvres in a multi-satellite mission environment. The study detailed the design of a gripper end effector, with particular emphasis on the description of contact mechanics between the end effector and interface.

A series of simulations was conducted using a multibody model that incorporated the environment, the robotic system and its control strategy, and the contact mechanics description. Simulations tested the influence of contact model parameters on the capture manoeuvre. Results demonstrated that the success of the manoeuvre is highly dependent on the stiffness of the contact materials, while the damping coefficient, related to the plastic deformation of materials, has negligible influence.

The findings allowed for the definition of a range of suitable materials for constructing the end effector and interface. The study concluded that stiffer materials such as aluminum, steel, or titanium were preferable, while polymeric or elastomeric materials are not suitable. The results indicated that the current end effector design can be constructed using common space-grade materials and can successfully perform berthing manoeuvres.

Future work will focus on developing a lumped parameter model to describe the contact mechanics to develop a digital twin of the system.

Acknowledgements

This research is coordinated and partially funded by the Italian Space Agency (Agenzia Spaziale Italiana, ASI) in the framework of the RESEARCH DAY "GIORNATE DELLA RICERCA ACCADEMICA SPAZIALE" initiative through the contract no. ASI-BVTECH-2023-2-E.0

References

[1] B. Yost and S. Weston, "State of the Art Small Spacecraft Technology," 2024. Accessed: Sep. 10, 2024. [Online]. Available: https://ntrs.nasa.gov/citations/20230005922

[2] E. Papadopoulos, F. Aghili, O. Ma, and R. Lampariello, "Robotic Manipulation and Capture in Space: A Survey," Jul. 19, 2021, *Frontiers Media S.A.* doi: 10.3389/frobt.2021.686723.

[3] W. Fehse, *Automated Rendezvous and Docking of Spacecraft*. Cambridge University Press, 2003. doi: 10.1017/CBO9780511543388.

[4] A. Flores-Abad, O. Ma, K. Pham, and S. Ulrich, "A review of space robotics technologies for on-orbit servicing," 2014, *Elsevier Ltd*. doi: 10.1016/j.paerosci.2014.03.002.

[5] Canadian Space Agency, "About Canadarm," https://www.asc-csa.gc.ca/eng/canadarm/about.asp.

[6] Canadian Space Agengy, "About Canadarm 2," https://www.asc-csa.gc.ca/eng/iss/canadarm2/about.asp.

[7] P. Laryssa *et al.*, "International Space Station Robotics: A Comparative Study of ERA, JEMRMS and MSS."

[8] European Space Agency, "European Robtic Arm," https://www.esa.int/Science_Exploration/Human_and_Robotic_Exploration/International_Space_Station/European_Robotic_Arm.

[9] D. Arney, J. Mulvaney, C. Williams, R. Sutherland, and C. Stockdale, "In-space Servicing, Assembly, and Manufacturing (ISAM) State of Play 2022 Edition."

[10] NASA, "OSAM-1 Mission," https://www.nasa.gov/mission/on-orbit-servicing-assembly-and-manufacturing-1/.

[11] NASA's Goddard Space Flight Center, "NASA's Robotic OSAM-1 Mission," https://www.nasa.gov/centers-and-facilities/goddard/nasas-robotic-osam-1-mission-completes-its-critical-design-review/.

[12] NASA, "OSAM-2 Mission," https://www.nasa.gov/mission/on-orbit-servicing-assembly-and-manufacturing-2-osam-2/.

[13] E. Tunstel, C. Thayer, B. Hayashi, and R. Saltus, "ModuLink: A Robotic Manipulation Applique for In-Space Servicing Vehicles," in *IEEE Aerospace Conference Proceedings*, IEEE Computer Society, 2023. doi: 10.1109/AERO55745.2023.10115712.

[14] P. Palmieri, M. Gaidano, M. Troise, L. Salamina, A. Ruggeri, and S. Mauro, "A deployable and inflatable robotic arm concept for aerospace applications," in *2021 IEEE International Workshop on Metrology for AeroSpace, MetroAeroSpace 2021 - Proceedings*, Institute of Electrical and Electronics Engineers Inc., Jun. 2021, pp. 453–458. doi: 10.1109/MetroAeroSpace51421.2021.9511654.

[15] P. Palmieri, M. Gaidano, A. Ruggeri, L. Salamina, M. Troise, and S. Mauro, "An Inflatable Robotic Assistant for Onboard Applications," in *Proceedings of the International Astronautical Congress, IAC*, International Astronautical Federation, IAF, 2021.

[16] X. L. Ding, Y. C. Wang, Y. B. Wang, and K. Xu, "A review of structures, verification, and calibration technologies of space robotic systems for on-orbit servicing," Mar. 01, 2021, *Springer Verlag*. doi: 10.1007/s11431-020-1737-4.

[17] A. Stolfi, P. Gasbarri, and A. K. Misra, "A two-arm flexible space manipulator system for post-grasping manipulation operations of a passive target object," *Acta Astronaut*, vol. 175, pp. 66–78, Oct. 2020, doi: 10.1016/j.actaastro.2020.04.045.

[18] K. Yoshida, H. Nakanishi, H. Ueno, N. Inaba, T. Nishimaki, and M. Oda, "Dynamics, control and impedance matching for robotic capture of a non-cooperative satellite," *Advanced Robotics*, vol. 18, no. 2, pp. 175–198, 2004, doi: 10.1163/156855304322758015.

[19] G. Gilardi and I. Sharf, "Literature survey of contact dynamics modelling." [Online]. Available: www.elsevier.com/locate/mechmt

[20] W. Cheng, L. Tianxi, and Z. Yang, "Grasping strategy in space robot capturing floating target," *Chinese Journal of Aeronautics*, vol. 23, no. 5, pp. 591–598, Oct. 2010, doi: 10.1016/S1000-9361(09)60259-4.

[21] S. Wu, F. Mou, Q. Liu, and J. Cheng, "Contact dynamics and control of a space robot capturing a tumbling object," *Acta Astronaut*, vol. 151, pp. 532–542, Oct. 2018, doi: 10.1016/j.actaastro.2018.06.052.

[22] O. Ma, G. Yang, and X. Diao, "EXPERIMENTAL VALIDATION OF CDT-BASED SATELLITE DOCKING SIMULATIONS USING SOSS TESTBED," 2005.

[23] J. Wang, R. Mukherji, M. Ficocelli, A. Ogilvie, and C. Rice, "Contact dynamics simulations for robotic servicing of Hubble Space Telescope," in *Modeling, Simulation, and Verification of Space-based Systems III*, SPIE, May 2006, p. 622103. doi: 10.1117/12.665348.

[24] Institute of Electrical and Electronics Engineers., *The proceedings of 2006 IEEE/RSJ International Conference on Intelligent Robots and Systems : IROS 2006 : Beijing, China, October 9-15, 2006*.

[25] L. Salamina, D. Botto, S. Mauro, and S. Pastorelli, "Modeling of flexible bodies for the study of control in the simulink environment," *Applied Sciences (Switzerland)*, vol. 10, no. 17, Sep. 2020, doi: 10.3390/app10175861.

[26] A. C. Bertolino, G. Jacazio, S. Mauro, and M. Sorli, "Developing of a Simscape Multibody Contact Library for Gothic Arc Ball Screws: A Three-Dimensional Model for Internal Sphere/Grooves Interactions," in *Volume 4: Dynamics, Vibration, and Control*, American Society of Mechanical Engineers, Nov. 2019. doi: 10.1115/IMECE2019-10709.

[27] A. Sapietová, L. Gajdoš, V. Dekýš, and M. Sapieta, "Analysis of the influence of input function contact Parameters of the impact force Process in the MSC. ADAMS," in *Advances in Intelligent Systems and Computing*, vol. 393, Springer Verlag, 2016, pp. 243–253. doi: 10.1007/978-3-319-23923-1_37.

[28] "Adams 2020 FP1 Adams View User's Guide," 2020. [Online]. Available: http://msc-documentation.questionpro.com.

[29] C. Verheul and S. International, "Benelux ADAMS User Meeting."

[30] P. Palmieri, M. Troise, L. Salamina, M. Gaidano, M. Melchiorre, and S. Mauro, "An Inflatable 7-DOF Space Robotic Arm for Active Debris Removal," in *Okada, M. (eds) Advances in Mechanism and Machine Science. IFToMM WC 2023. Mechanisms and Machine Science, vol 148*, Springer, Cham, 2023, pp. 580–589. doi: 10.1007/978-3-031-45770-8_58.

[31] P. Palmieri, M. Troise, M. Gaidano, M. Melchiorre, and S. Mauro, "Inflatable Robotic Manipulator for Space Debris Mitigation by Visual Servoing," in *2023 9th International Conference on Automation, Robotics and Applications, ICARA 2023*, Institute of Electrical and Electronics Engineers Inc., 2023, pp. 175–179. doi: 10.1109/ICARA56516.2023.10125753.

[32] B. Siciliano, L. Sciavicco, L. Villani, and G. Oriolo, *Robotics. Modelling, Planning and Control*. 2010.